Volume-Law to Area-Law Entanglement Transition in a Nonunitary Periodic Gaussian Circuit

Etienne Granet and Carolyn Zhang
Department of Physics, Kadanoff Center for Theoretical Physics, University of Chicago, Chicago, Illinois 60637, USA

Henrik Dreyer
Quantinuum, Leopoldstrasse 180, 80804 Munich, Germany

(Received 11 January 2023; accepted 26 April 2023; published 8 June 2023)

We consider Gaussian quantum circuits that alternate unitary gates and postselected weak measurements, with spatial translation symmetry and time p eriodicity. We show analytically that such models can host different kinds of measurement-induced phase transitions detected by entanglement entropy, by mapping the unitary gates and weak measurements onto Möbius transformations. We demonstrate the existence of a log-law to area-law transition, as well as a volume-law to area-law transition at a finite measurement amplitude. For the latter, we compute the critical exponent ν for the Hartley, von Neumann and Rényi entropies exactly.

DOI: 10.1103/PhysRevLett.130.230401

Introduction.—In recent years, there has been an immense amount of work on dynamical phase transitions driven by competition between unitary time evolution and projective measurements, called measurement-induced phase transitions (MIPTs). Although generic unitary time evolution leads to volume-law entangled states in the long-time limit, interspersing the unitary evolution with local measurements can stabilize area-law entangled steady states [1–4]. These MIPTs have been studied in various setups, mostly through numerical methods [5–31]. A subclass of circuits called Gaussian circuits allows for analytical calculations because they only involve unitaries and measurements built out of fermion bilinears. However, though the volume-law to area-law MIPT was observed for interacting circuits, it has not yet been observed in Gaussian circuits [32–39].

In this Letter, we analytically study Gaussian nonunitary circuits with spatial translation symmetry and discrete time translation symmetry. They consist of Gaussian unitary gates and weak measurements, obtained by coupling the system to ancillas, measuring the ancillas, and postselecting [40]. We show that these nonunitary circuits can demonstrate MIPTs between different entanglement phases as we tune the measurement amplitude, which is related to the ancilla coupling. Surprisingly, for specific parameters, we find a volume-law to area-law transition at a finite measurement amplitude. We derive the exact critical measurement amplitude and the correlation length exponents $\{\nu_n\}$ for the Hartley ($n = 0$), von Neumann ($n = 1$) and Rényi ($n > 1$) entanglement entropies. To our knowledge, this is the first example of a volume-law to area-law transition in a Gaussian nonunitary circuit, and of an analytical computation of all $\{\nu_n\}$ at a MIPT.

Setup.—We study nonunitary circuits built out of the following translation-invariant 1D layers [41,42]:

$$U_{ZZ}(t) = e^{-it\sum_{j=1}^{L}\sigma_j^z\sigma_{j+1}^z},$$
$$U_{YY}(t) = e^{-it\sum_{j=1}^{L}\sigma_j^y\sigma_{j+1}^y},$$
$$U_X(t) = e^{-it\sum_{j=1}^{L}\sigma_j^x}, \tag{1}$$

where $\sigma_j^{x,y,z}$ are Pauli matrices, and periodic boundary conditions $L + 1 \equiv 1$ are assumed. These layers can be written as free fermion evolution using the standard Jordan-Wigner transformation $\sigma_j^x = 1\text{–}2c_j^\dagger c_j$ and $\sigma_j^z = (c_j + c_j^\dagger)\prod_{\ell=1}^{j-1}(1 - 2c_\ell^\dagger c_\ell)$, where $c_j^\dagger, c_j$ are fermion

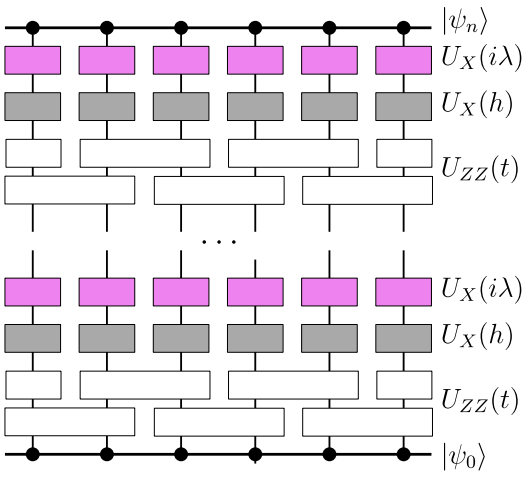

FIG. 1. A schematic of n applications of the round described by (3), with $p = 1$. $|\psi_n\rangle$ is the normalized final state.

 © 2023 American Physical Society

creation and annihilation operators. Nonunitarity is introduced by allowing t to be complex, which corresponds to weak measurement [40] or dynamics in open quantum systems [43].

We will focus on circuits built out of the following elementary cycle of layers

$$U(t,h,\lambda) = U_X(i\lambda)U_X(h)U_{ZZ}(t), \tag{2}$$

for t, h, λ real parameters. We can use this cycle to build more complicated rounds described by $\mathcal{U}$:

$$\mathcal{U} = U(t_p,h_p,\lambda_p)\ldots U(t_1,h_1,\lambda_1), \tag{3}$$

with $t_r, h_r, \lambda_r, r \in \{1,\ldots,p\}$ fixed real parameters. We will study the entanglement properties of a subsystem of large size ℓ after $n \to \infty$ identical rounds $\mathcal{U}$, in the thermodynamic limit $L \to \infty$, with $\ell \ll n \ll L$. This kind of setup, for $p = 1$, is illustrated in Fig. 1. Because each round is identical, our models have discrete time translation symmetry. While we use the particular structure of cycle and round defined in (2) and (3), we note that our methods can be applied to any round built out of (1).

Time evolution via Möbius transformations.—The actions of the layers in (1) are particularly simple on coherent states [41]. These are states of the form

$$|\psi(\mathcal{A},f(k))\rangle = \mathcal{A}\prod_{k\in K_L^+}[1+f(k)c^\dagger(-k)c^\dagger(k)]|0\rangle, \tag{4}$$

where $K_L = (2\pi/L)\{-(L/2)+\frac{1}{2},\ldots,(L/2)-\frac{1}{2}\}$ and $K_L^+ \subset K_L$ contains all the positive momenta, and $|0\rangle$ the tensor product of $+1$ eigenstates of σ_j^x at each site. Here, $\mathcal{A}$ normalizes the state and contains a phase, and $f(k)$ is an amplitude for fermions at momenta $k, -k$.

The crucial observation of Ref. [41] was that a coherent state remains a coherent state after the application of any of the layers in (1), but with modified $\mathcal{A}$ and $f(k)$. In particular, each of the layers in (1) transforms $f(k)$ by a Möbius transformation:

$$U_g(t)|\psi(\mathcal{A},f(k))\rangle = |\psi(\tilde{\mathcal{A}},\tilde{f}(k))\rangle, \tag{5}$$

where $g = ZZ, YY, X$ and

$$\tilde{f}(k) = F(f) = \frac{af(k)+b}{cf(k)+d}, \tag{6}$$

where a, b, c, and d are complex functions of t and k. We provide their explicit forms for the three kinds of layers in the Supplemental Material [40]. The transformation on $\mathcal{A}$ will not be needed in this work. Because the composition of Möbius transformations is a Möbius transformation, the action of $U(t,h,\lambda)$ and $\mathcal{U}$ can also be written as (6). It follows that $\mathcal{U}^n|\psi(\mathcal{A},f(k))\rangle$ also produces a coherent state for any n. Like any Möbius transformation, the transformation associated with $\mathcal{U}$ can be packaged into a 2×2 matrix

$$\mathcal{M}_k = \begin{pmatrix} a & b \\ c & d \end{pmatrix} \tag{7}$$

acting on the vector $\binom{f(k)}{1}$: the new value $\tilde{f}(k)$ is given by the ratio of the two components of the resulting vector. The matrix of the Möbius transformation associated with $\mathcal{U}^n$ is then simply obtained by repeated matrix multiplications $\mathcal{M}_k^n$. Therefore, in order to obtain the behavior at large n of $\mathcal{U}^n|0\rangle$, we need to study the fixed points of the Möbius transformation $\mathcal{M}_k$ associated with $\mathcal{U}$ and their stability. Note that the initial state can be any coherent state, and therefore any free fermion state with zero total momentum, as well as some nonzero momentum states by applying with $c^\dagger(k_0)$ operators on the coherent state [44].

Let us denote the normalized state after n rounds by $|\psi(\mathcal{A}_n,f_n(k))\rangle$. The fixed points of the Möbius transformation are the two solutions to the quadratic equation

$$f_\infty(k) = \frac{af_\infty(k)+b}{cf_\infty(k)+d}. \tag{8}$$

We label these fixed points by $f_\infty^-(k)$ and $f_\infty^+(k)$ for each k. The stability of these fixed points are given by $|F'(f)|$: if $|F'(f)|_{f=f_\infty^-(k)} < 1$, then $f_\infty^-(k)$ is a stable fixed point. Since a Möbius transformation can have at most only one stable fixed point, any choice of initial state $f_0(k) \neq f_\infty^+(k)$ will be attracted to $f_\infty^-(k)$ as $n \to \infty$, for that particular value of k. It can be shown that

$$|F'(f)|_{f=f_\infty^-} = \frac{1}{|F'(f)|_{f=f_\infty^+}} = \frac{|\mu_-(k)|}{|\mu_+(k)|}, \tag{9}$$

where $\mu_-(k)$ and $\mu_+(k)$ with $|\mu_-(k)| \leq |\mu_+(k)|$ are the two eigenvalues of $\mathcal{M}_k$. So for $|\mu_-(k)| \neq |\mu_+(k)|$, there is a unique stable fixed point given by $f_\infty^-(k)$, while $f_\infty^+(k)$ is an unstable fixed point. On the contrary, if $|\mu_-(k)| = |\mu_+(k)|$, then there are no stable fixed points and $f_n(k)$ will not converge as $n \to \infty$ whenever $f_0(k) \neq f_\infty^\pm(k)$.

These two alternatives completely determine the steady state entanglement properties. Let us call the values of k for which $|\mu_-(k)| = |\mu_+(k)|$ "critical." We will only need to consider $k \in [0,\pi]$ because $f(k)$ must be an antisymmetric function for (4) to be consistent. If there are no critical $k \in [0,\pi]$, we will show that the steady state has area-law entanglement, which in 1D means that in the thermodynamic limit $S_m(\ell)$ saturates to a finite value when $\ell \to \infty$. If there is a finite number of critical k, then the steady state generically has log-law entanglement: $S_m(\ell) \sim \log(\ell)$.

Finally, if there is a whole interval of critical k, then the steady state has volume-law entanglement: $S_m(\ell) \sim \ell$.

In order to determine analytically whether such critical k exist for a given Möbius transformation, we use that $|\mu_-(k)| = |\mu_+(k)|$ if and only if the following two conditions are satisfied:

$$(i)\ \Im \frac{\mathrm{Tr}(\mathcal{M}_k)}{\sqrt{\det(\mathcal{M}_k)}} = 0 \quad (ii)\ \left|\Re \frac{\mathrm{Tr}(\mathcal{M}_k)}{\sqrt{\det(\mathcal{M}_k)}}\right| \leq 2. \tag{10}$$

We prove this in the Supplemental Material [40]. We will now give two examples of nonunitary circuits and show that, by studying their corresponding Möbius transformations, we can obtain their phase diagrams exactly.

Log-law to area-law transition.—We will now show that a log-law to area-law transition can occur in a simple circuit containing only one cycle (2), i.e., $p = 1$ in (3). For this circuit, we have

$$\mathcal{M}_k = \begin{pmatrix} z_{k,t} e^{-2\lambda+2ih} & e^{-2\lambda+2ih} \\ -e^{2\lambda-2ih} & z_{k,t}^* e^{2\lambda-2ih} \end{pmatrix}, \tag{11}$$

where

$$z_{k,t} = \frac{e^{2it}\tan(k/2) + \frac{e^{-2it}}{\tan(k/2)}}{2\sin(2t)}. \tag{12}$$

To investigate the entanglement properties of this circuit, we study the conditions (10) for the existence of critical k, as detailed in the Supplemental Material [40]. We find that if $\lambda = 0$, both conditions in (10) are satisfied for all k. Because there is a whole interval of critical k (in fact, the entire range of k), the steady state exhibits volume-law entanglement, as expected in absence of measurements. For $\lambda > 0$, the phase of the system depends on the condition $|\tan(2h)| > |\tan(2t)|$. If this condition holds, then the steady state always demonstrates area-law entanglement. Otherwise, there is a critical value λ_c such that for $0 < \lambda < \lambda_c$ there is a unique critical k given by $k = \arccos[\tan(2h)/\tan(2t)]$ for which both conditions of (10) hold, implying a log-law entanglement. For $\lambda > \lambda_c$ there are no critical k, indicating area-law entanglement. $\lambda_c(t,h)$ can be computed exactly and is given in the Supplemental Material [40]. Therefore, when $|\tan(2h)| < |\tan(2t)|$, the system demonstrates a log-law to area-law transition at $\lambda = \lambda_c$. Such transitions are well known in free fermionic nonunitary circuits [33,35,45,46].

Let us finally mention the case $h = t = \pi/4$. Here we find for any λ an interval $[k_c, \pi - k_c]$ of critical k, with $0 < k_c < \pi/2$ depending on λ. This yields a volume law phase, but without any transition to an area-law behavior at any finite λ, consistent with Ref. [47].

Volume-law to area-law transition.—We now consider a round with two cycles:

$$\mathcal{U} = U(t_2, h_2, \lambda) U(t_1, h_1, \lambda). \tag{13}$$

For generic values of the parameters, such circuits do not have volume-law to area-law MIPTs in λ. However, for

$$t_1 = h_1 = \frac{\pi}{4} - x, \qquad t_2 = h_2 = \frac{\pi}{4} + x, \tag{14}$$

where $x \in [0, \pi/4]$, we will show that there exists an x-dependent λ_c such that the steady state demonstrates volume-law entanglement for $\lambda < \lambda_c$ and area-law entanglement for $\lambda > \lambda_c$.

From the definition of $z_{k,t}$ in (12), we have $z_{k,t_1} = -z_{k,t_2}^*$. Therefore, $\mathcal{M}_k$ for (13) simplifies to

$$\mathcal{M}_k = \begin{pmatrix} |z_{k,t_1}|^2 e^{-4\lambda} - e^{4ix} & z_{k,t_1}^*(e^{-4\lambda} + e^{4ix}) \\ -z_{k,t_1}(e^{4\lambda} + e^{-4ix}) & |z_{k,t_1}|^2 e^{4\lambda} - e^{-4ix} \end{pmatrix}. \tag{15}$$

To determine the critical k, we compute

$$\frac{\mathrm{Tr}(\mathcal{M}_k)}{\sqrt{\det(\mathcal{M}_k)}} = 2\frac{|z_{k,t_1}|^2 \cosh(4\lambda) - \cos(4x)}{1 + |z_{k,t_1}|^2}. \tag{16}$$

This quantity is always real, so condition (i) of (10) is satisfied for all k. Condition (ii) can be written as

$$\tan^2(k/2) + \frac{1}{\tan^2(k/2)} \leq \frac{4\cos^4(2x)}{\sinh^2(2\lambda)} + 2\cos(4x). \tag{17}$$

For this to hold for at least one value of k, we need it to be true for $k = \pi/2$, which minimizes the left-hand side. Plugging in $k = \pi/2$, we find that the interval of critical k disappears when $\lambda > \lambda_c$, where

$$\lambda_c = \frac{1}{2}\mathrm{arcsinh}\left[\frac{\cos^2(2x)}{\sin(2x)}\right]. \tag{18}$$

Therefore, the steady state demonstrates area-law entanglement for $\lambda > \lambda_c$. For $\lambda < \lambda_c$, (17) is satisfied for $k \in [k_c, \pi - k_c]$, with k_c obeying (17) with equality. Within this interval, $f_n(k)$ does not converge to a stable fixed point, and we will now show that this leads to volume-law entanglement.

Behavior of entanglement entropy.—Given a state $|\psi\rangle$ on a spin chain of size L, the reduced density matrix ρ_ℓ on $[1, \ell]$ is given by

$$\rho_\ell = \mathrm{Tr}_{\ell+1,\ldots,L}(|\psi\rangle\langle\psi|). \tag{19}$$

We define the entanglement entropies $S_m(\ell)$ as

$$\begin{aligned} S_0(\ell) &= \log \text{rank}[\rho], \qquad \text{Hartley} \\ S_1(\ell) &= -\text{Tr}[\rho \log \rho], \qquad \text{von Neumann} \\ S_m(\ell) &= \frac{\log \text{Tr}[\rho^m]}{1-m}, \qquad m \geq 2, \qquad \text{Rényi}. \end{aligned} \tag{20}$$

While it is difficult to obtain the exact behavior of $S_m(\ell)$ at intermediate times, we can compute the coefficient of the volume-law ($\mathcal{O}(\ell)$) contribution to $S_m(\ell)$ in the $n \to \infty$ limit. To that end, we introduce the correlation matrix Γ on the subsystem $[1, 2, \ldots \ell]$, given by

$$\langle \psi | \begin{pmatrix} a_{2j-1} \\ a_{2j} \end{pmatrix} \cdot \begin{pmatrix} a_{2k-1} & a_{2k} \end{pmatrix} | \psi \rangle = \delta_{j,k} + i\Gamma_{jk}, \tag{21}$$

with the Majorana fermions $a_{2j-1} = c_j + c_j^\dagger$ and $a_{2j} = i(c_j - c_j^\dagger)$. Γ has a block-Toeplitz structure:

$$\Gamma = (\Pi_{j-i})_{i,j=1,\ldots,\ell} \qquad \Pi_j = \begin{pmatrix} -\varphi_j & \psi_j \\ -\psi_{-j} & \varphi_j \end{pmatrix}, \tag{22}$$

where from (4), φ_j and ψ_j are computed to be

$$\begin{aligned} \varphi_j &= \frac{i}{2\pi} \int_{-\pi}^{\pi} dk e^{-ikj} \frac{f_n(k) + f_n(k)^*}{1 + |f_n(k)|^2} \\ \psi_j &= \frac{1}{2\pi} \int_{-\pi}^{\pi} dk e^{-ikj} \frac{f_n(k) - f_n(k)^* + |f_n(k)|^2 - 1}{1 + |f_n(k)|^2}. \end{aligned} \tag{23}$$

We find that φ_j and ψ_j converge to some $\bar{\varphi}_j$ and $\bar{\psi}_j$ respectively as $n \to \infty$, and we define $\hat{\varphi}(k)$ and $\hat{\psi}(k)$ through $\bar{\varphi}_j = (1/2\pi) \int_{-\pi}^{\pi} dk e^{-ikj} \hat{\varphi}(k)$ and $\bar{\psi}_j = (1/2\pi) \int_{-\pi}^{\pi} dk e^{-ikj} \hat{\psi}(k)$. When $f_n(k)$ converges to a stable fixed point, we can replace $f_n(k)$ in (23) by $f_\infty^-(k)$. Notice that if there is a critical value of k, then $f_\infty^-(k)$ generically fails to be smooth because it jumps between the two fixed points of the Möbius transformation. This leads to power-law decay of correlations of Majorana fermions in real-space according to (23), implying log-law entanglement. On the other hand, if there are no critical k, $f_\infty^-(k)$ is smooth and real-space correlations decay exponentially, implying area-law entanglement for pure states [48,49].

If $k \in [k_c, \pi - k_c]$ is critical, then $f_n(k)$ in this momentum range does not converge and depends on both the initial state $f_0(k)$ and the cycle number n. We choose the initial state $f_0(k) = 0$ for all k which, in the spin language, means all spins in the $+1$ eigenstate of σ_j^x. For this initial state, we have $f_n(k) = x_n(k)/y_n(k)$ with

$$\begin{pmatrix} x_n(k) \\ y_n(k) \end{pmatrix} = \mathcal{M}_k^n \cdot \begin{pmatrix} 0 \\ 1 \end{pmatrix}. \tag{24}$$

Since $|\mu_-(k)| = |\mu_+(k)|$, we can write $\mu_+(k)/\mu_-(k) = e^{2i\theta_k}$ for $k \in [k_c, \pi - k_c]$, where

$$\theta_k = \arccos\left[\frac{|z_{k,t_1}|^2 \cosh(4\lambda) - \cos(4x)}{1 + |z_{k,t_1}|^2}\right]. \tag{25}$$

Diagonalizing $\mathcal{M}_k$, we find

$$f_n(k) = \frac{b(k) \sin(n\theta_k)}{(-a(k) + \cos\theta_k)\sin(n\theta_k) + \sin(\theta_k)\cos(n\theta_k)}, \tag{26}$$

where a and b are matrix elements of $\mathcal{M}_k/\sqrt{\det \mathcal{M}_k}$ as in (7), and we have indicated their k dependence explicitly. We see that in this case, $f_n(k)$ does not converge to a stable fixed point as $n \to \infty$ and instead keeps oscillating. To compute $\hat{\varphi}(k)$ and $\hat{\psi}(k)$, we separate the slowly varying and quickly oscillating parts of $f_n(k)$ by defining

$$\mathfrak{f}(k, u) = \frac{b(k) \sin u}{(-a(k) + \cos\theta_k)\sin u + \sin\theta_k \cos u}. \tag{27}$$

As shown in the Supplemental Material [40] we compute $\hat{\varphi}(k)$ and $\hat{\psi}(k)$ by averaging over the fast oscillations:

$$\begin{aligned} \hat{\varphi}(k) &= \frac{i}{2\pi} \int_0^{2\pi} du \frac{\mathfrak{f}(k,u) + \mathfrak{f}(k,u)^*}{1 + |\mathfrak{f}(k,u)|^2}, \\ \hat{\psi}(k) &= \frac{1}{2\pi} \int_0^{2\pi} du \frac{\mathfrak{f}(k,u) - \mathfrak{f}(k,u)^* + |\mathfrak{f}(k,u)|^2 - 1}{1 + |\mathfrak{f}(k,u)|^2}. \end{aligned} \tag{28}$$

We now follow Ref. [50] to compute the entanglement entropy. Repeating the calculations therein, we find the following leading behavior when $\ell \to \infty$:

$$S_m(\ell) = \frac{\ell}{2\pi} \int_{-\pi}^{\pi} dk H_m\left(\sqrt{|\hat{\varphi}(k)|^2 + |\hat{\psi}(k)|^2}\right), \tag{29}$$

with $\mathcal{O}(\log \ell)$ corrections, and with $H_m(x)$ given by

$$\begin{aligned} H_0(x) &= \mathbb{1}_{x \in (-1,1)}, \\ H_1(x) &= -\frac{1+x}{2}\log\frac{1+x}{2} - \frac{1-x}{2}\log\frac{1-x}{2}, \\ H_m(x) &= \frac{1}{1-m}\log\left[\left(\frac{1+x}{2}\right)^m + \left(\frac{1-x}{2}\right)^m\right], \end{aligned} \tag{30}$$

for $m \geq 2$. When $f_n(k)$ converges to a stable fixed point, we plug $f_\infty^-(k)$ into the definition of $\hat{\varphi}(k)$ and $\hat{\psi}(k)$, and obtain

$$|\hat{\varphi}(k)|^2 + |\hat{\psi}(k)|^2 = 1. \tag{31}$$

Since $H_m(1) = 0$, these momenta do not contribute to the volume law term $\mathcal{O}(\ell)$, nor to the $\mathcal{O}(\log \ell)$ term [51].

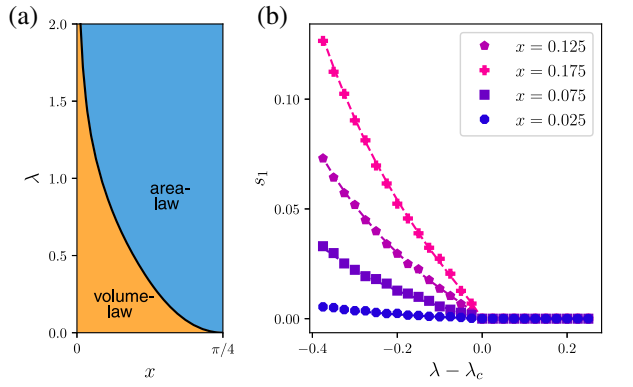

FIG. 2. (a) Phase diagram for the nonunitary circuit described in (13), with x and λ as defined in (14) and (2), respectively. The phase boundary is given by (18). (b) Scaling of the von-Neumann entropy. Markers denote the slope of the best linear fits to the exact entropy $S_1(\ell) \sim s_1\ell + b$ after 500 cycles on subsystem sizes up to $\ell = 100$. Dashed lines denote the closed form expression (29).

On the other hand, when $f_n(k)$ does not converge to a stable fixed point, we can show from (27) that [40]

$$|\hat{\varphi}(k)|^2 + |\hat{\psi}(k)|^2 < 1. \tag{32}$$

Therefore, these momenta do contribute to the $\mathcal{O}(\ell)$ term. We obtain

$$S_m(\ell) = \begin{cases} s_m(\lambda)\ell, & \text{if } \lambda < \lambda_c \\ \mathcal{O}(\ell^0), & \text{if } \lambda > \lambda_c, \end{cases} \tag{33}$$

with $s_m(\lambda)$ a coefficient computable from (29) (see Supplemental Material [40]). We compare these exact calculations with numerical computations of entanglement entropies in Fig. 2. In the limit $\lambda \to \lambda_c$, we define the critical exponent ν by the leading behaviour of $s_m(\lambda)$ when $\lambda \to \lambda_c$:

$$s_m(\lambda) = a_m(\lambda_c - \lambda)^\nu + \mathcal{O}[(\lambda_c - \lambda)^{\nu'}], \tag{34}$$

where $\nu' > \nu$. We obtain analytically

$$\begin{aligned} s_0(\lambda_c - \lambda) &\sim (\lambda_c - \lambda)^{1/2} \\ s_1(\lambda_c - \lambda) &\sim (\lambda_c - \lambda)\log(\lambda_c - \lambda) \\ s_m(\lambda_c - \lambda) &\sim (\lambda_c - \lambda), \end{aligned} \tag{35}$$

with coefficients given in the Supplemental Material [40] and subleading terms $\sim(\lambda_c - \lambda)^{3/2}$. Therefore, $\nu = \frac{1}{2}$ for $S_0(\ell)$ and $\nu = 1$ for $S_m(\ell)$, where $m \geq 1$, with marginal logarithmic corrections at $m = 1$ [52,53]. At the critical point $\lambda = \lambda_c$, the only critical k is $k = \pi/2$, but $\theta_{\pi/2} = 0$ according to (25). So $f_n(\pi/2)$ converges to a stationary value, and the $\mathcal{O}(\log\ell)$ coefficients vanish, yielding a central charge $c = 0$, consistent with Refs. [35,46].

Discussion.—We presented a general framework for obtaining exact results on steady states of clean Gaussian nonunitary circuits with discrete time translation symmetry using Möbius transformations. A few comments are in order. First, it was shown in Refs. [8,37] that entanglement transitions are also purification transitions. This can also be seen in our analysis: if a Möbius transformation has a single stable fixed point for all k, the steady state is independent of the initial state. Therefore, the corresponding circuit would map mixed states to the pure state given by $f_\infty^-(k)$, as $n \to \infty$. On the other hand, when there is a region of critical k, $f_n(k)$ in this interval always retains its dependence on the initial state, and a mixed state remains mixed even as $n \to \infty$.

Second, we note that the distinction governed by conditions (10) is equivalent to a statement on the reality of the single-particle energies $\{\epsilon_k\}$ of the effective Hamiltonian H defined by $\mathcal{U} = e^{iH}$: ϵ_k is real if and only if k is critical. Therefore, increasing the nonunitarity of the model through λ has a similar effect as in the continuous-time model of Ref. [31].

While we only studied steady states of two simple kinds of rounds, the general framework of Möbius transformations can be used to study any other circuit built out of the layers in (1) and their intermediate time dynamics. Note that these MIPTs can be detected directly by either measuring two-point correlation functions in the steady state or by measuring correlations between mode occupation numbers $c^\dagger(k)c(k)$. For the latter, the measurement outcome depends on the criticality of k. Therefore, while difficult to implement due to the midcircuit postselection, they are easy to detect.

C. Z. thanks David Huse, Tim Hsieh, and Soonwon Choi for helpful discussions. E. G. thanks Adam Nahum and Lorenzo Piroli for interesting discussions. C. Z. acknowledges support from the University of Chicago Bloomenthal Fellowship and the National Science Foundation Graduate Research Fellowship under Grant No. 1746045. E. G. acknowledges support from the Kadanoff Center for Theoretical Physics at University of Chicago, and from the Simons Collaboration on Ultra-Quantum Matter.

[1] B. Skinner, J. Ruhman, and A. Nahum, Phys. Rev. X **9**, 031009 (2019).
[2] Y. Li, X. Chen, and M. P. A. Fisher, Phys. Rev. B **98**, 205136 (2018).
[3] Y. Li, X. Chen, and M. P. A. Fisher, Phys. Rev. B **100**, 134306 (2019).
[4] A. Chan, R. M. Nandkishore, M. Pretko, and G. Smith, Phys. Rev. B **99**, 224307 (2019).
[5] M. Szyniszewski, A. Romito, and H. Schomerus, Phys. Rev. B **100**, 064204 (2019).
[6] A. Zabalo, M. J. Gullans, J. H. Wilson, S. Gopalakrishnan, D. A. Huse, and J. H. Pixley, Phys. Rev. B **101**, 060301(R) (2020).

[7] S. Choi, Y. Bao, X.-L. Qi, and E. Altman, Phys. Rev. Lett. **125**, 030505 (2020).
[8] M. J. Gullans and D. A. Huse, Phys. Rev. X **10**, 041020 (2020).
[9] S.-K. Jian, C. Liu, X. Chen, B. Swingle, and P. Zhang, Phys. Rev. Lett. **127**, 140601 (2021).
[10] A. Nahum, S. Roy, B. Skinner, and J. Ruhman, PRX Quantum **2**, 010352 (2021).
[11] M. Buchhold, Y. Minoguchi, A. Altland, and S. Diehl, Phys. Rev. X **11**, 041004 (2021).
[12] Q. Tang and W. Zhu, Phys. Rev. Res. **2**, 013022 (2020).
[13] S. Gopalakrishnan and M. J. Gullans, Phys. Rev. Lett. **126**, 170503 (2021).
[14] X. Turkeshi, R. Fazio, and M. Dalmonte, Phys. Rev. B **102**, 014315 (2020).
[15] M. Block, Y. Bao, S. Choi, E. Altman, and N. Y. Yao, Phys. Rev. Lett. **128**, 010604 (2022).
[16] U. Agrawal, A. Zabalo, K. Chen, J. H. Wilson, A. C. Potter, J. H. Pixley, S. Gopalakrishnan, and R. Vasseur, Phys. Rev. X **12**, 041002 (2022).
[17] S. Sang, Y. Li, T. Zhou, X. Chen, T. H. Hsieh, and M. P. A. Fisher, PRX Quantum **2**, 030313 (2021).
[18] M. Szyniszewski, A. Romito, and H. Schomerus, Phys. Rev. Lett. **125**, 210602 (2020).
[19] S. Goto and I. Danshita, Phys. Rev. A **102**, 033316 (2020).
[20] O. Lunt and A. Pal, Phys. Rev. Res. **2**, 043072 (2020).
[21] T. Botzung, S. Diehl, and M. Müller, Phys. Rev. B **104**, 184422 (2021).
[22] J. Lopez-Piqueres, B. Ware, and R. Vasseur, Phys. Rev. B **102**, 064202 (2020).
[23] C. Noel, P. Niroula, D. Zhu, A. Risinger, L. Egan, D. Biswas, M. Cetina, A. V. Gorshkov, M. J. Gullans, D. A. Huse *et al.*, Nat. Phys. **18**, 760 (2022).
[24] J. Iaconis, A. Lucas, and X. Chen, Phys. Rev. B **102**, 224311 (2020).
[25] Z.-C. Yang, Y. Li, M. P. A. Fisher, and X. Chen, Phys. Rev. B **105**, 104306 (2022).
[26] Y. Bao, S. Choi, and E. Altman, Phys. Rev. B **101**, 104301 (2020).
[27] C.-M. Jian, Y.-Z. You, R. Vasseur, and A. W. W. Ludwig, Phys. Rev. B **101**, 104302 (2020).
[28] B. Bertini and L. Piroli, Phys. Rev. B **102**, 064305 (2020).
[29] T.-C. Lu and T. Grover, PRX Quantum **2**, 040319 (2021).
[30] K. Klobas and B. Bertini, SciPost Phys. **11**, 107 (2021).
[31] Y. Le Gal, X. Turkeshi, and M. Schiro, arXiv:2210.11937.
[32] X. Cao, A. Tilloy, and A. De Luca, SciPost Phys. **7**, 024 (2019).
[33] X. Chen, Y. Li, M. P. A. Fisher, and A. Lucas, Phys. Rev. Res. **2**, 033017 (2020).
[34] A. Nahum and B. Skinner, Phys. Rev. Res. **2**, 023288 (2020).
[35] O. Alberton, M. Buchhold, and S. Diehl, Phys. Rev. Lett. **126**, 170602 (2021).
[36] C.-M. Jian, B. Bauer, A. Keselman, and A. W. W. Ludwig, Phys. Rev. B **106**, 134206 (2022).
[37] L. Fidkowski, J. Haah, and M. B. Hastings, Quantum **5**, 382 (2021).
[38] F. Carollo and V. Alba, Phys. Rev. B **106**, L220304 (2022).
[39] P. Zhang, S.-K. Jian, C. Liu, and X. Chen, Quantum **5**, 579 (2021).
[40] See Supplemental Material at http://link.aps.org/supplemental/10.1103/PhysRevLett.130.230401 for details.
[41] H. Dreyer, M. Bejan, and E. Granet, Phys. Rev. A **104**, 062614 (2021).
[42] E. Granet, H. Dreyer, and F. H. Essler, SciPost Phys. **12**, 019 (2022).
[43] A. McDonald, R. Hanai, and A. A. Clerk, Phys. Rev. B **105**, 064302 (2022).
[44] E. Granet, arXiv:2209.08756.
[45] M. Ippoliti, T. Rakovszky, and V. Khemani, Phys. Rev. X **12**, 011045 (2022).
[46] X. Turkeshi, A. Biella, R. Fazio, M. Dalmonte, and M. Schiró, Phys. Rev. B **103**, 224210 (2021).
[47] T.-C. Lu and T. Grover, PRX Quantum **2**, 040319 (2021).
[48] M. B. Hastings, J. Stat. Mech. (2007) P08024.
[49] F. G. Brandao and M. Horodecki, Commun. Math. Phys. **333**, 761 (2015).
[50] P. Calabrese and J. Cardy, J. Stat. Mech. (2005) P04010.
[51] F. Ares, J. G. Esteve, F. Falceto, and Z. Zimborás, J. Stat. Mech. (2019) 093105.
[52] I. Affleck, D. Gepner, H. J. Schulz, and T. Ziman, J. Phys. A **22**, 511 (1989).
[53] S. Eggert, Phys. Rev. B **54**, R9612 (1996).